Metallophysics and Advanced Technologies
Металофіз. новітні технол.
Metallofiz. Noveishie Tekhnol.
2022, vol. 44, No. 1, pp. 19–30
https://doi.org/10.15407/mfint.44.01.0019
Reprints available directly from the publisher

CRYSTAL-LATTICE DEFECTS

PACS numbers: 61.72.Mm, 68.35.bd, 68.35.Rh, 81.10.Fq, 81.30.Kf

Regularities of Grain Structure Formation in Thin Ribbons of Iron–Nickel Alloy

V. J. Bondar, P. Yu. Volosevich, V. Yu. Danilchenko, and Ie. M. Dzevin

G. V. Kurdyumov Institute for Metal Physics, N.A.S. of Ukraine,
36 Academician Vernadsky Blvd.,
UA-03142 Kyiv, Ukraine

The regularities of the grain structure formation of the austenitic phase in the ribbon of the metastable iron–nickel alloy Fe–31.4% wt. Ni–0.05% wt. C, formed in the conditions of high temperature gradients during quenching from the melt and its influence on the realization of martensitic γ–α-transformation in the local regions of the formed ribbon are investigated. The dependence of the completeness of the martensitic transformation and morphology of martensite crystals on the grain size of austenite is analysed. The change in the relative intensity of the diffraction reflexes of the γ-phase lines along the depth of the ribbon is characterized by a continuous change in the degree of austenite texture. The consequences of the influence of relaxation processes during the crystallization of the ribbon on the value of residual stresses, the presence of triple 120° joints between the grains as signs of equilibrium, and the change in their number along the ribbon are investigated.

Key words: martensitic transformation, austenite, solid solution, spinning, crystal structure, diffraction.

Досліджено закономірності формування зеренної структури аустенітної фази у стрічці метастабільного залізо-нікелевого стопу Fe–31,4% ваг. Ni–0,05% ваг. C, сформованої в умовах високих температурних ґрадієнтів у разі гартування з розтопу, та її вплив на реалізацію мартенситного γ–α-перетворення у локальних областях сформованої стрічки. Проаналізована залежність повноти реалізації мартенситного перетворення та морфології мартенситних кристалів від розміру зерна аустеніту. За зміною від-

Corresponding author: Vitaliy Yuhymovych Danilchenko
E-mail: danila@imp.kiev.ua

Citation: V. J. Bondar, P. Yu. Volosevich, V. Yu. Danilchenko, and Ie. M. Dzevin, Regularities of Grain Structure Formation in Thin Ribbons of Iron–Nickel Alloy, *Metallofiz. Noveishie Tekhnol.*, **44**, No. 1: 19–30 (2022).
DOI: 10.15407/mfint.44.01.0019

носної інтенсивності дифракційних рефлексів ліній γ-фази по глибині стрічки характеризували безперервну зміну ступеня текстури аустеніту. Досліджено наслідки впливу релаксаційних процесів у разі кристалізації стрічки на величину залишкових напружень, наявність потрійних 120° стиків між зернами, як ознаки рівноважного стану та зміну їх кількості вздовж стрічки.

Ключові слова: мартенситне перетворення, аустеніт, твердий розчин, спінінгування, кристалічна структура, дифракція.

(Received November 15, 2021)

1. INTRODUCTION

One of the most relevant areas of modern materials science is the development of metallic materials with special properties by ultra-fast hardening of the melt (spinning). Due to cooling at a rate of (10^6–10^8)°C/s in such materials a specific structural-phase state is formed, macro- and micro-inhomogeneities appear, phase components are crushed (refined), the region of mutual solubility of chemical elements is significantly expanded [1–4].

This leads to the formation of a new set of physical and mechanical and operational properties of fast-quenched alloys. In this regard, intensive research and development of highly dispersed metallic materials has been carried out for the last 20 years.

The main factor influencing the change in the properties of fast-quenched materials is the grain size of the phase components. Metal materials with an ultrafine (grain size—100–1000 nm) or nanocrystalline (grain size—20–100 nm) structure are obtained by quenching of the liquid melt. It is impossible to obtain such fine-grained grain by traditional methods of heat treatment. Fast-quenched materials can be considered as qualitatively new perspective materials of the next generation. They can be used as structural, instrumental and functional materials. In the nanocrystalline state alloys have increased strength, hardness, low thermal conductivity, high grain boundary diffusion coefficient and improved magnetic characteristics. Further progress in the development of fast-hardened alloys is associated with the purposeful control of the processes of their non-equilibrium crystallization and structural-phase transformations in the solid state.

Additional possibilities of controlling the structure formation of thin-film materials from metastable iron-based alloys appear in the course of martensitic transformations (MP), which are realized in the process of ultrafast crystallization of the melt or in the subsequent cooling and external factors. There is a certain prospect of creating new materials based on fast-quenched iron–nickel alloys, in which direct γ–α- and reverse α–γ-MP occur during cooling and subsequent

heating [5–7]. The complex effect of fast-quenched alloys can be significantly affected by the dimensional effect of MP, which is that when the size of the austenitic grain decreases, the temperature of the beginning of transformation decreases, the amount of martensite and the size of martensite crystals decrease [8–10].

However, the powerful MP factor can be used to form a new set of properties of metastable alloys only if we study the features of such transformations in thin-film materials obtained in sharply non-equilibrium conditions of superfast cooling. Thus, the study of the features of MP and regularities of formation of the structural-phase state in the local regions of thin ribbons of metastable alloys based on iron, fast-quenched from the melt, are important and relevant.

In this work a study of the peculiarities of the grain structure formation of austenite in the local regions of a thin ribbon of metastable iron–nickel alloy, fast-quenched from the melt, and its effect on the characteristics of MP during subsequent cooling have been carried out.

2. MATERIALS AND METHODS

The object used in the study is a ribbon obtained from iron–nickel alloy N31 (31.4% wt. Ni; 0.05% wt. C). It is obtained in a carbon dioxide atmosphere at a cooling rate of (10^5–10^6) °C/s. A continuous ribbon with a thickness of 30 μm and a width of 8 mm is obtained by spinning of 100 g of melt by casting its flat jet on the outer surface of a massive copper drum, which rotated at a speed of 4000 rpm [11]. At room temperature the ribbon is in an austenitic state. Under cooling in liquid nitrogen, the direct γ–α-MP is realized. The heating in a salt bath with temperatures between 450–500°C leads to reverse α–γ-transformation.

X-ray studies are performed on an automated diffractometer DRON-3 using a graphite monochromator in iron and cobalt radiation. Residual stresses are measured by the non-destructive X-ray method $\sin^2\psi$, which is based on the measurement of elastic deformation of the crystal lattice [12]. Measurements are performed by the austenitic reflex $(311)_\gamma$ with sequential rotation of the sample at angles of 10°, 15°, 20°, 25°, 30°. The accuracy of stress measurement is ±20 MPa.

The grain structure of the ribbon is studied along the contact and free surfaces, as well as in the planes of oblique longitudinal and cross sections on an optical microscope MIM-7. Etching of the sections is performed in an electrolyte solution (glycerol—10%, perchloric acid—20%, ethyl alcohol—70%) at a voltage of 3 V. For better wetting of the surfaces of the sections in the electrolyte solution a small amount of surfactant is added. Metallographic observations of structures on the free and contact surfaces of the ribbon are performed without prior mechanical grinding and etching, and sections of oblique longitudinal and cross sections are etched in a similar manner. In order to observe

the microstructure of the cross section 4–7 ribbons 2–3 cm long are glued with epoxy resin into bags, which after curing are cut at an angle of about 45 degrees and ground with a fine abrasive and polished using chromium oxide powder. Electrolytic etching of such sections is performed in a solution of perchloric acid according to the mode: voltage 10 V, time—10 s. The average grain diameter is determined from 30 metallographic images containing more than 300 grains. Image-Pro Plus (MediaCedernetics, Inc.) is used to determine grain sizes.

Samples for electron microscopic studying of the ribbon on a JEM-200CX transmission electron microscope are prepared without prior mechanical treatment by electrolytic polishing in a solution of 25 g of chromic anhydride in 75 ml of glacial acetic acid and 10 ml of distilled water under cooling with running water. The polishing mode is in the range $U = 90–100$ V, $I = 0.8–1$ A.

Measurements of the microhardness of the ribbon are performed on the device PMT-3 under load on the indenter 25 and 65 g. A diamond pyramid with an angle between the faces of 136° is used as an indenter.

3. RESULTS OF EXPERIMENTS AND DISCUSSION

Metallographic studies revealed a significant heterogeneity of the grain structure of the ribbon. There is a significant difference in grain size on the contact and free surfaces, as well as in sections on the width and length of the austenitic ribbon. Most of the austenite grains on the free surface of the ribbon had a shape close to equilibrium. On the contact surface, the grains had a shape elongated in the direction of rotation of the drum. The elongated shape of the grains on the contact surface is not transmitted to the free surface of the ribbon.

The ribbon is inhomogeneous in thickness. The difference in thickness at the edges (periphery) and in the middle of the ribbon reached 4 μm. The thickness at the end of the ribbon is less than 3 μm compared to the beginning of the ribbon. Deviations from the average thickness of the ribbon are associated with a decrease in the adhesion of the ribbon to the surface of the drum due to its heating by a liquid jet.

On the free side, the predominant number (more than 30%) are grains with a size of 2 μm, and about 10% had a size of 0.3 μm or less. On the contact side, about 40% of the grains had a size of 1.0–1.8 μm and about 16% had a size less than 0.2 μm. Intermediate-sized grains are observed in the volume (oblique section) of the ribbon.

Due to the gradual heating of the drum surface in the ribbon developed thermally activated relaxation processes, which resulted in almost complete absence of residual stresses along its entire length of the ribbon. Tensions are absent at the beginning of the formation of the ribbon. This meant that the formation of the austenitic structure of the ribbon occurred under conditions of relaxation processes as the

surface of the drum is heated.

A certain number of triple joints of grains with angles between the boundaries close to 120° are observed (Fig. 1). Analysis of the evolution of triple intergranular joints in the formation of the ribbon allows us to conclude about the development of recrystallization processes as a result of gradual heating of the cooler disk with a liquid melt [13]. At the initial stage of forming the ribbon (cold drum), the angles between the sides of the triple joints differed from 120° by (2–4)°, and as the drum heated, this difference decreased, and at the end of the ribbon (warm disk) the angles differed by no more than two degrees. In parallel with this process, the number of triple joints increased, as well as the number of adjacent such joints increased. The successive manifestation of these stages of formation of the grain structure, which contained triple joints of grains, testified to the gradual development of relaxation processes during the formation of the ribbon.

Samples cut from different parts of the ribbon showed an increase in grain size as they approached the end of the ribbon. At the end of the ribbon, when the drum is noticeably heated, the grain size increased to 4–5 μm due to a decrease in the degree of supercooling.

The heterogeneity of the grain structure determined different values of microhardness in different areas of the contact and free sides of the ribbon. The decrease in the size of the austenitic grains on the contact side led to an increase in the microhardness in the central part by 24 kg/mm^2 compared to the free side (Fig. 2). In addition, the edge effect is observed along the width of the ribbon—on the periphery of the ribbon the microhardness is increased by 18 kg/mm^2 compared to the central section (Fig. 2). Increased microhardness of the ribbon in the austenitic state is recorded in areas with smaller austenitic grains.

The amount of martensitic phase, determined by the X-ray method in relation to the integral intensity of reflexes $(111)_\gamma/(110)_\alpha$, is significantly different on the contact and free surfaces, as well as on the

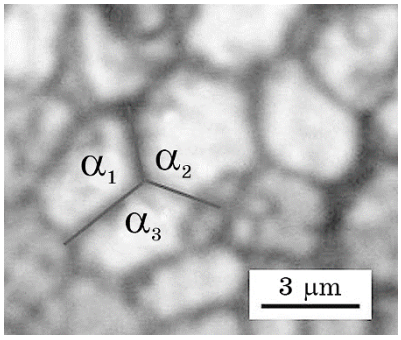

Fig. 1. The 120° boundaries at the joints of three grains (end of the ribbon), angles between grain boundaries: α_1—118°, α_2—121°, α_3—121°.

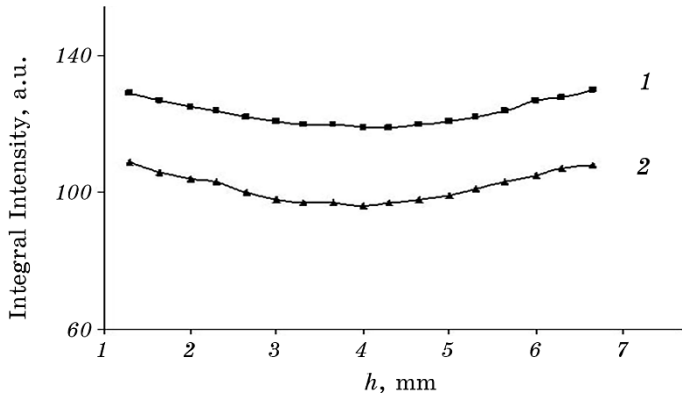

Fig. 2. Change in the microhardness of the ribbon (γ-state) obtained on the cold drum, in width (*1*, *2* are the contact and free side, respectively).

width and along the ribbon. 60% of martensite is formed on the contact surface, and up to 88% on the free surface. Along the ribbon, towards its end, the amount of martensite increased in accordance with the increase in the size of austenitic grains. The difference in the amount of martensite at the beginning and end of the ribbon reached 11% (on the contact surface). These changes in the amount of martensite are completely determined by the dimensional effect of MP.

Electron microscopic studies showed that the structural state of austenitic grains gradually changed during the formation of the ribbon. Accordingly, the structural state of the martensitic phase formed in such grains during the subsequent cooling of the ribbon in liquid nitrogen also changed.

The results of studies of the structural features of the ribbon at its beginning and end after cooling in liquid nitrogen are shown in Figs. 3 and 4. Their analysis shows that in austenite grains with a diameter less than 1.2 μm (Fig. 3, *a*, *b*) MP after cooling in liquid nitrogen is practically not realized (beginning of the ribbon). Inhibition of MP in small austenitic grains of fast-quenched alloys is previously observed in [14]. Martensite crystals with different morphological features (needle and massive) are formed in larger grains (Fig. 3, *c*, *d*). The use of a dark-field image allowed to observe the micro-twinned structure of martensite (Fig. 3, *d*).

The increase in the size of martensite crystals is accompanied by the appearance inside them of signs of micro-twinning, which is confirmed by the analysis of electron diffraction pattern and conducted dark-field studies (Fig. 4, *d*, *e*). In grains with a diameter less than 2 μm MP is inhibited, and the amount of residual austenite increased. This is evidenced by the presence on the electron diffraction pattern of reflexes of the $(200)_\gamma$ type (Fig. 4, *b*). The internal structure of massive mar-

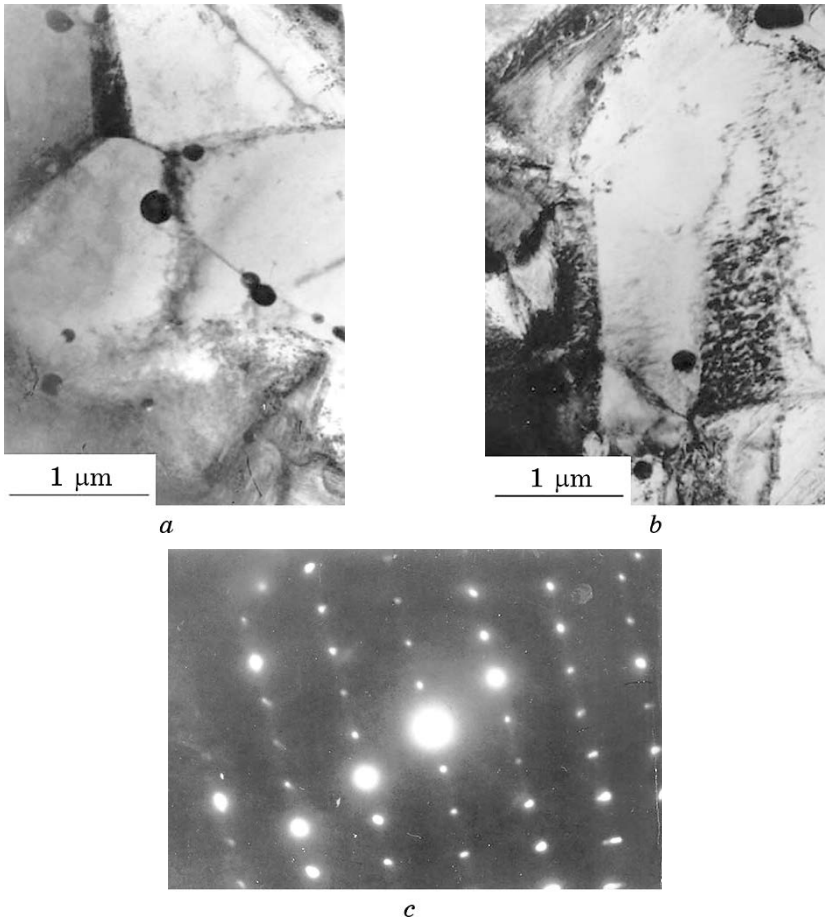

Fig. 3. The microstructures of the ribbon obtained on the cold drum, after cooling in liquid nitrogen (*a*, *b*) and the electron diffraction pattern (*c*) from the area shown in (*b*).

tensite and small-sized needle martensite crystals had a dislocation character. These results are consistent with the conclusions of [15–18], which showed that the thickness of the sample and the place of origin of the martensitic phase determine its morphological features.

The density of dislocations in martensitic crystals of both morphologies is in the range of 10^{11} cm^{-2}. Austenite grains with a diameter more than 3 μm in the vast majority are converted almost completely into martensite. In grains with a diameter of less than 1.5 μm MP is inhibited, and the amount of residual austenite increased. This is evidenced by the presence on the electron diffraction pattern of reflexes of the $(200)_\gamma$ type (Fig. 4, *b*).

The ribbon obtained on the warm drum contained austenitic grains

much larger (up to 5 μm) in average size compared to the grains at its beginning (1 μm). In such large grains, the amount of needle martensite with predominantly dislocation (Fig. 4, *a*) or dislocation and micro-twinned (Fig. 4, *d*) internal structures approached 100%. The crystals of martensite with microtwins are much larger while maintaining the same morphological features.

In [9] to explain the dimensional effect of MP from the size of austenitic grains in thin ribbons of Fe–Ni alloys obtained by melt quenching, we used the concept of critical average of austenitic grain size, in which MP is completely inhibited. Our experiments showed that this is observed in almost all grains of a certain size. The general regularity is that the completeness of the MP decreased with decreasing austenitic grain size. In [9] it is noted that MP is observed in much smaller grains

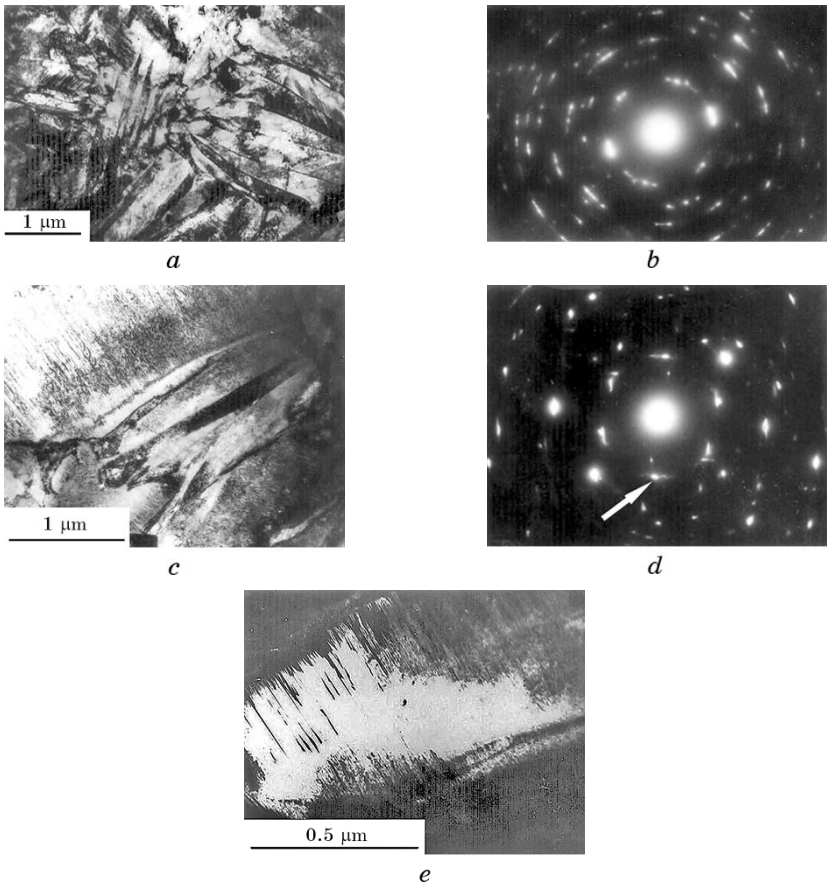

Fig. 4. The microstructures of the ribbon obtained on the warm drum, after cooling in liquid nitrogen (*a*, *c*) and the dark field image (*e*) obtained with (*c*) in the reflex indicated on the electron diffraction pattern (*d*) by the arrow.

and at the same time in some larger grains MP is not realized. This contradiction can be explained by taking into account that the structural state (dislocation density, presence of fragments with small angular boundaries, internal stresses and distribution of alloying elements) can differ significantly and depend on heat treatment, including for the same grains, especially in the range of close to critical. It is the structural state of austenitic grains and their environment could contribute to the transformation into small grains. The author of [10] also previously came to the conclusion that the concept of critical average austenitic grain size, introduced in [9], is devoid of physical meaning.

Analysis of diffraction patterns from different local areas of the ribbon showed a pronounced texture of the structure of austenite on the free surface. On the contact surface the intensity ratio of the austenitic reflexes I_{200}/I_{111} along the ribbon varied from 0.8 to 0.7, and for the free surface from 4.5 to 5.8 (Table 1). The diffraction pattern from the free surface reflected the growth texture $\langle 100 \rangle$, characteristic of the f.c.c. structure. On the contact side the texture is much less.

On the contact surface this texture is expressed much less (Table 2). The degree of texturing markedly varied in width and length of the ribbon in accordance with the change in cooling rate during the crystallization of the ribbon. On the free surface of the ribbon observed a certain distribution of the texture ratio I_{200}/I_{111} and the width of the ribbon. On the contact surface these values did not change.

TABLE 1. The relative intensity of diffraction reflexes of austenite along the surfaces along the length of the ribbon (γ-state).

The surface of the ribbon	A section of ribbon	$I_{200\gamma}/I_{111\gamma}$
Contact	The beginning	0.8
	The middle	0.72
	The end	0.7
Free	The beginning	4.5
	The middle	5.1
	The end	5.8

TABLE 2. The ratio of the integrated intensity of austenitic and martensitic reflexes on the contact and free surfaces at the beginning and end of the quenched ribbon from the alloy N31 after cooling in liquid nitrogen ($\gamma + \alpha$-state).

The surface of the ribbon	A section of ribbon	$I_{200\alpha}/I_{110\alpha}$	$I_{211\alpha}/I_{110\alpha}$	$I_{110\alpha}/I_{111\gamma}$
Contact	The beginning	0.11	0.87	1.8
	The middle	0.12	0.88	1.2
	The end	0.13	0.93	5.7
Free	The beginning	0.12	0.92	6.6

Additional information about the texture of the ribbon can give X-ray of the surface of the ribbon at different inclinations of the primary X-ray beam. In this diffraction mode reflexes are formed at different depths, which are determined by the magnitude of the angle of inclination [18]. The monotonic decrease in the integral intensity of all major austenitic reflexes in depth indicated the absence of texture in the near-surface layer from the contact surface (Fig. 5, *a*). From the free surface, the intensity of the reflex $(220)_\gamma$ changed along the curve with a maximum at a beam inclination of about 40° (Fig. 5, *b*). This indicated the possibility of changing the type of texture in the near-surface layer up to 3–5 μm thick from the free surface (inner texture). The regularity of the formation of the internal texture deserves a special study.

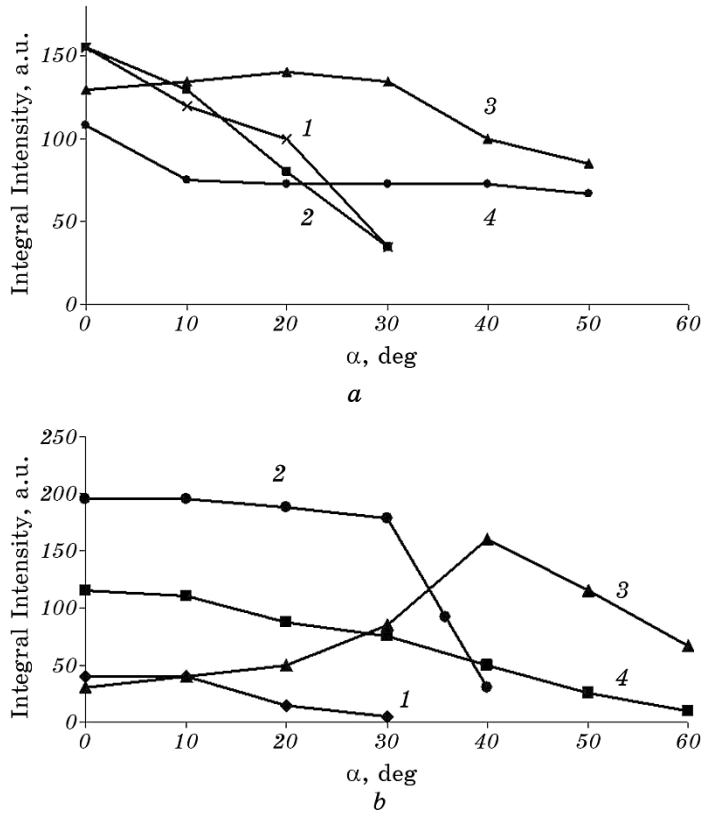

Fig. 5. Dependence of the integral intensity of austenitic reflexes on the angle of inclination relative to the Bragg position for each of the reflexes: *1*—$(111)_{K\alpha}$, $2\theta = 33{,}97°$, *2*—$(200)_{K\alpha}$, $2\theta = 39{,}95°$, *3*— $(220)_{K\alpha}$, $2\theta = 64{,}98°$, *4*—$(311)_{K\beta}$, $2\theta = 74{,}95°$. *a*—free side, *b*—contact side.

4. CONCLUSIONS

The formation of dimensional parameters of austenitic grains and their internal structure along the ribbon of fast-hardened alloy Fe–31.4% wt. Ni–0.05% wt. C took place under the conditions of relaxation processes, which are associated with the gradual heating of the cooling drum by the melt jet. As a result, the structural state and properties changed along the ribbon. This simultaneously ensured the absence of residual stresses in the austenitic phase along the entire length of the ribbon and an increase in grain size from 1–2 μm at the beginning of the ribbon to 4–5 μm at its end due to a decrease in the degree of supercooling. In addition, the relaxation processes resulted in the formation of triple 120° joints of grain boundaries (a sign of recrystallization) and an increase in the number of such adjacent boundaries along the ribbon.

On the free side of the thin ribbon, a one-sided axial texture of the growth of the $\langle 100 \rangle$ austenitic phase, characteristic of the f.c.c. structure, is formed. The degree of texture varied across the width and along the ribbon according to the change in cooling rate. On the contact side, the texture is less pronounced.

The internal structure of martensite crystals formed in austenitic grains of different sizes is formed by one or two types of defects in the crystal structure—dislocations and microtwins. Microtwins together with dislocations are observed in larger martensite crystals, and in small crystals the morphology is mainly dislocation.

REFERENCES

1. I. S. Miroshnichenko, *Zakalka iz Zhidkogo Sostoyaniya* [Quenching from Liquid State] (Moscow: Metallurgiya: 1982) (in Russian).
2. A. Inoue, Y. Kojima, T. Minemura, and T. Masumoto, *Trans. Iron Steel Inst. Jpn.*, **21**, No. 9: 656 (1981).
3. S. Zaichenko and A. Glezer, *Interface Sci.*, **7**: 57 (1999).
4. A. Glezer, E. Blinova, V. Pozdnyakov, and A. Shelyakov, *J. Nanoparticle Res.*, **5**: 551 (2003).
5. L. I. Lysak and B. I. Nikolin, *Fizicheskie Osnovy Termicheskoy Obrabotki Stali* [Physical Bases of the Thermal Treatment of Steel] (Kyiv: Tekhnika: 1975) (in Russian).
6. G. V. Kurdyumov, *Voprosy Fiziki Metallov i Metallovedeniya*, No. 3: 9 (1952) (in Russian).
7. A. L. Roitburd, *Mater. Sci. Eng. A*, **127**, No. 2: 229 (1990).
8. K. Yamauchi and Y. Yoshihito, *Mater. Sci. Forum*, **225–227**: 781 (1996).
9. E. N. Blinova, A. M. Glezer, V. A. Diakonova, and V. A. Zorin, *Izv. RAN, Physics*, **65**, No. 10: 1444 (2001).
10. V. A. Lobodyuk, *Phys. Met. Metallogr.*, **99**, Iss. 2: 143 (2005) (in Russian).
11. V. K. Nosenko, *Formirovanie Amorfnykh i Nanokristallicheskikh Sostoyaniy v*

Splavakh na Osnove Fe i Al [Formation of Amorphous and Nanocrystalline States in the Alloys on Fe and Al Base] (PhD Thesis) (Kyiv: G. V. Kurdyumov Institute for Metal Physics N.A.S.U.: 2005) (in Russian).
12. N. I. Komyak and U. G. Myasnikov, *Rentgenovskie Metody i Oborudovanie dlya Opredeleniya Napryazheniy* [X-ray Methods and Equipment for Stresses Determination] (Leningrad: Mashinostroenie: 1972) (in Russian).
13. Ch. V. Kopeckij, A. N. Orlov, and L. K. Fionova, *Granitsy Zyeren v Chistykh Materialakh* [The Grain Boundaries in Pure Materials] (Moscow: Nauka: 1987) (in Russian).
14. P. Yu. Volosevych, S. Yu. Makarenko, A. V. Proshak, V. E. Panarin, M. Ye. Svavil'nyi, and V. I. Bondarchuk, *Metallofiz. Noveishie Tekhnol.*, **42**, No. 1: 51 (2020) (in Ukrainian).
15. V. I. Izotov and P. A. Handarov, *FMM*, **34**, No. 2: 332 (1972) (in Russian).
16. P. Yu. Volosevich, V. N. Gridnev, and Yu. N. Petrov, *Metallofizika*, No. 62: 71 (1975) (in Russian).
17. P. Yu. Volosevich, *Physics, Chemistry and Mechanics of Surfaces*, **8**, No. 12: 1648 (1992).
18. L. I. Mirkin, *Rentgenovskiy Analiz Polikristallov* [X-ray Analisys of Polycrystals] (Moscow: 1961) (in Russian).